

# Pressure-enhanced superconductivity and upper critical field in $\text{Sr}_{0.5}\text{Pr}_{0.5}\text{FBiS}_2$

Lin Li<sup>1</sup>, Yongliang Xiang<sup>1</sup>, Jianliang Xu<sup>1</sup>, Minling Zhou<sup>1</sup>, Li

Zhang<sup>2</sup>, Xiaofeng Xu<sup>1</sup>, Chao Cao<sup>1</sup>, Jianhui Dai<sup>1</sup>, Yuke Li<sup>1,\*</sup>

<sup>1</sup>*Department of Physics and Hangzhou Key Laboratory of Quantum Matter,  
Hangzhou Normal University, Hangzhou 310036, China*

<sup>2</sup>*Department of Physics, China Jiliang University, Hangzhou 310018, China*

(Dated: October 30, 2015)

Through a combination of X-ray diffraction, electrical transport, and magnetic susceptibility measurements, we report a newly BiS<sub>2</sub>-based  $\text{Sr}_{0.5}\text{Pr}_{0.5}\text{FBiS}_2$  superconductor with  $T_c$  of 2.7 K at ambient pressure. Upon applying pressure,  $T_c$  is abruptly enhanced, reaches 8.5 K at a critical pressure of  $P_c = 1.5$  GPa and remains a slight increase up to 9.7 K up to 2.5 GPa. Accompanied with the enhancement of superconductivity from the low- $T_c$  phase to the high- $T_c$  phase, the normal state undergoes a semiconductor to metal transition under pressure. Meanwhile, the upper critical field ( $B_{c2}(0)$ ) is substantially enhanced in excess of the Pauli paramagnetic limit. Phase diagram in terms of temperature versus pressure for  $\text{Sr}_{0.5}\text{Pr}_{0.5}\text{FBiS}_2$  is thus obtained.

PACS numbers: 74.70.Xa; 74.25.F-; 74.62.Fj; 74.25.Dw

## I. INTRODUCTION

The discovery of superconductivity with  $T_c$  of 8.6 K<sup>1</sup> in a layered crystal structure compound  $\text{Bi}_4\text{O}_4\text{S}_3$  has evoked considerable attention. Following this work, many BiS<sub>2</sub>-based superconductors including  $\text{LnO}_{1-x}\text{F}_x\text{BiS}_2$  ( $\text{Ln}=\text{La}, \text{Ce}, \text{Pr}, \text{Nd}$ )<sup>2–6</sup> with the highest  $T_c$  of  $\sim 10$  K have been then reported and studied. Similar to the copper oxide and iron-based superconductors with alternating stacks of superconducting and blocking layers, the crystal structure of BiS<sub>2</sub>-based compounds is composed of the common superconducting BiS<sub>2</sub> layers intercalated by various block layers, e.g.,  $\text{Bi}_4\text{O}_4(\text{SO}_4)_{1-x}$  or  $[\text{Ln}_2\text{O}_2]^{2-}$ . Subsequently, another family of BiS<sub>2</sub>-based superconductors  $\text{Sr}_{1-x}\text{Ln}_x\text{FBiS}_2$  ( $\text{Ln}=\text{La}, \text{Ce}$ ) with the tetragonal crystal structure has been synthesized and investigated.<sup>7,8</sup> The parent compound  $\text{SrFBiS}_2$  is a band insulators without detectable antiferromagnetic transition or structure phase transition.<sup>9,10</sup> Superconductivity with  $T_c$  of  $\sim 2.8$  K has been induced by rare earth elements La or Ce doping into lattice, but its normal state exhibits the semiconducting-like behaviors even if in the optimal superconducting sample.<sup>5,11</sup> Most studies on the BiS<sub>2</sub>-based system have mainly focused on the effect of chemical substitution and superconducting transition temperature<sup>12</sup> so far.

Pressure is considered as a clean method for adjusting the lattice parameter and the electronic band structure, which can enhance superconductivity and tune the normal state behaviors. Among the BiS<sub>2</sub>-based superconductors,  $\text{LaO}_{1-x}\text{F}_x\text{BiS}_2$  shows superconductivity at about  $T_c = 2.6$  K at ambient pressure, but its  $T_c$  reaches a maximum value of  $\sim 10$  K at  $P = 2$  GPa.<sup>13</sup> The finding seems to be an universal feature, which is also observed in most BiS<sub>2</sub>-based superconductors with a dramatic enhancement of  $T_c$  under pressure.<sup>13–15</sup> The reason may be hinted by X-ray diffraction measurements which indicate that the system undergoes a structural phase transition from a tetragonal phase to a monoclinic phase at a criti-

cal pressure.<sup>16</sup> The suppression of semiconducting behavior through increasing the carriers density was claimed to contribute the enhanced superconductivity.<sup>17</sup> In addition, Hall effect measurements of  $\text{Eu}_3\text{F}_4\text{Bi}_2\text{S}_4$  reveal a change in electronic structures across the superconducting phase under pressure.<sup>15</sup> Up to now,  $\text{Sr}_{1-x}\text{Ln}_x\text{FBiS}_2$  ( $\text{Ln} = \text{rare earth elements}$ ), as the newly discovered BiS<sub>2</sub>-based family, has exhibited the unique properties but is less investigated.<sup>7</sup> An interesting observation is that the La doping can induce a semiconductor to metal transition in the  $\text{Sr}_{0.5}\text{La}_{0.5}\text{FBiS}_2$  system, accompanied with a sign changed Hall coefficient, even though its band structure is similar to that of  $\text{LaO}_{1-x}\text{F}_x\text{BiS}_2$ .<sup>10</sup> In  $\text{Sr}_{0.5}\text{Ce}_{0.5}\text{FBiS}_2$ , the diluted-Ce ions order ferromagnetically at about 7.5 K, and coexist with superconductivity below 2.8 K.<sup>8</sup> The study of substitution effect for other magnetic rare earth elements in  $\text{SrFBiS}_2$  system is high desirable, in particular for pressure effect on the superconductivity and the normal state properties.

In the paper, we report the successful synthesis of a newly Pr-doped  $\text{Sr}_{0.5}\text{Pr}_{0.5}\text{FBiS}_2$  superconductor, and the detailed high-pressure effect on superconductivity and its normal state properties. We found that  $\text{Sr}_{0.5}\text{Pr}_{0.5}\text{FBiS}_2$  displays superconductivity at 2.7 K at ambient pressure. Upon the increase of applied pressure,  $T_c$  is abruptly enhanced, reaching 8.5 K at a critical pressure of  $P_c = 1.5$  GPa, and then increases slightly to 9.7 K up to 2.5 GPa. Accompanied with the enhancement of superconductivity, the normal state resistivity undergoes a semiconductor to metal transition under pressure. Meanwhile, the upper critical field ( $B_{c2}(0)$ ) is substantially enhanced in excess of Pauli paramagnetic limit. Its value at high pressure is over ten times larger than that at ambient pressure. The ratio of  $B_{c2}(0)/T_c$  dramatically increases from 0.7 T/K at  $P = 0$  to 2.6 T/K at  $P = 2.5$  GPa, in contrast to that observed in the isostructural  $\text{EuFBiS}_2$ . According to those data, the phase diagram of temperature dependence of pressure for  $\text{Sr}_{0.5}\text{Pr}_{0.5}\text{FBiS}_2$  is thus established.

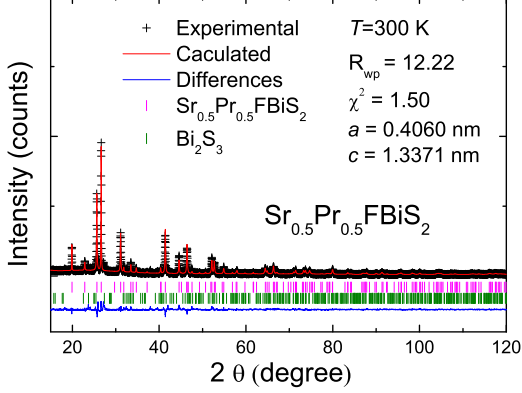


FIG. 1. (color online). Powder X-ray diffraction patterns and the Rietveld refinement profile for  $\text{Sr}_{0.5}\text{Pr}_{0.5}\text{FBiS}_2$  samples at room temperature. The # peak positions designate the impurity phase of  $\text{Bi}_2\text{S}_3$ .

## II. EXPERIMENT

The polycrystalline samples of  $\text{Sr}_{0.5}\text{Pr}_{0.5}\text{FBiS}_2$  were synthesized by two-step solid state reaction method. The detailed synthesis methods can be found in the previous literature.<sup>7</sup> Crystal structure characterization was performed by powder X-ray diffraction (XRD) at room temperature using a D/Max-rA diffractometer with  $\text{CuK}\alpha$  radiation and a graphite monochromator. Lattice parameters were obtained by Rietveld refinements. The (magneto)resistivity under several magnetic fields was performed with a standard four-terminal method covering temperature range from 0.5 to 300 K in a commercial Quantum Design PPMS-9 system with a  $^3\text{He}$  refrigeration insert. The temperature dependence of d.c. magnetization was measured on a Quantum Design SQUID-VSM-7T. Measurement of resistivity under pressure was performed up to 2.5 GPa on PPMS-9T by using HPC-33 Piston type pressure cell with the Quantum Design DC resistivity and AC transport options. Hydrostatic pressures were generated by a BeCu/NiCrAl clamped piston-cylinder cell. The sample was immersed in a pressure transmitting medium (Daphne Oil) covered with a Teflon cell. Annealed Au wires were affixed to contact surfaces on each sample with silver epoxy in a standard four-wire configuration.

## III. RESULTS AND DISCUSSION

### A. Crystal structure and superconductivity

Figure 1 shows the powder XRD patterns and the result of the Rietveld structural refinement for the  $\text{Sr}_{0.5}\text{Pr}_{0.5}\text{FBiS}_2$  sample. Overall, main diffraction peaks

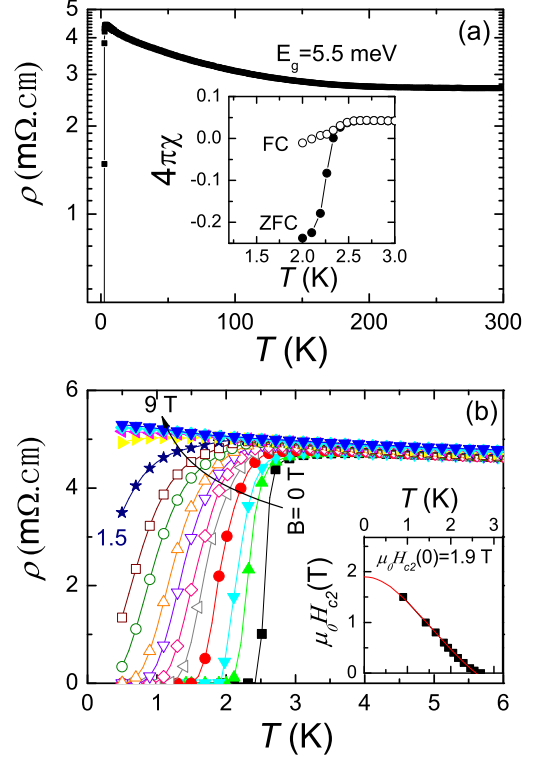


FIG. 2. (color online). (a) Temperature dependence of resistivity ( $\rho$ ) for the  $\text{Sr}_{0.5}\text{Pr}_{0.5}\text{FBiS}_2$  samples. The inset shows the diamagnetic signal vs. Temperature under a magnetic field of 5 Oe with ZFC (Solid) and FC (Open) modes. (b) An enlarged plot of resistivity around  $T_c$  under various magnetic fields. The inset shows temperature dependence of the upper critical field.

in the sample can be well indexed based on a  $\text{ZrCuSiAs}$ -type crystal structure with the  $P4/nmm$  space group. Extra tiny peaks arising from impurity phase of  $\text{Bi}_2\text{S}_3$  with  $Pnma$  symmetry can be observed,<sup>18</sup> and its content estimated by the Rietveld refinement is less than 5%. The refined lattice constants are extracted to be  $a = 4.0602\text{\AA}$  and  $c = 13.371\text{\AA}$ , both of them are smaller than those of parent compound  $\text{SrFBiS}_2$ .<sup>7</sup> As a result, the cell volume has a significant decrease. The remarkable shrink in lattice parameters indicates the successful substitution of Sr by Pr, similar to the case of Ce-doped in  $\text{Sr}_{0.5}\text{Ce}_{0.5}\text{FBiS}_2$  system.<sup>8</sup>

The temperature dependence of resistivity ( $\rho$ ) in  $\text{Sr}_{0.5}\text{Pr}_{0.5}\text{FBiS}_2$  is mapped in the main plane of figure 2(a). The resistivity exhibits a sharp superconducting transition below 2.7 K, followed by a semiconducting-like character in the normal state. The feature seems to be universal in the  $\text{BiS}_2$ -based superconductors,<sup>2,5</sup> but its nature still remains an open issue so far. By fitting with the thermal activation formula  $\rho(T) = \rho_0 \exp(E_a/k_B T)$  for the temperature range from 120 K to 300 K, the ther-

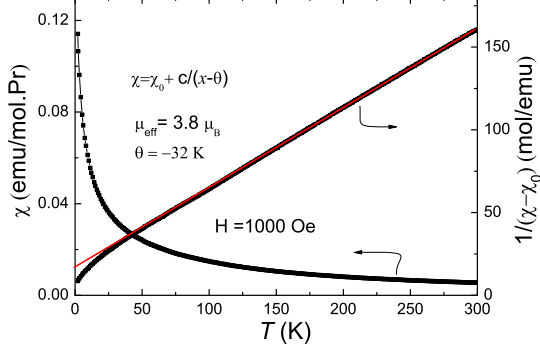


FIG. 3. (color online). The temperature dependent magnetic susceptibility under 1000 Oe magnetic field with FC modes for  $\text{Sr}_{0.5}\text{Pr}_{0.5}\text{FBiS}_2$  sample

mal activation energy ( $E_a$ ) obtained is about 5.5 meV, which is much smaller compared with the parent compound  $\text{SrFBiS}_2$  with 38.2 meV, implying the decrease of gap size due to electron doping.<sup>7</sup> It should be noted that the  $\text{Sr}_{0.5}\text{Pr}_{0.5}\text{FBiS}_2$  sample in the previous literature<sup>19</sup> superconductivity was not reported at ambient pressure. To determine the bulk superconductivity in our sample, the d.c. magnetic susceptibility with both zero field cooling (ZFC) and field cooling (FC) modes under 5 Oe is shown in the inset of figure 2(a). Below  $T_c$ , the strong diamagnetic signal can be clearly observed. From ZFC data, the estimated volume fraction of superconducting shielding is close to 30%, confirming the bulk superconductivity. The relatively small volume fraction is commonly found in the  $\text{BiS}_2$ -based polycrystalline samples, which is ascribed to the sample preparation method leading to a low- $T_c$  phase.<sup>2,20</sup>

Figure 2(b) shows a plot of  $\rho(T)$  under various magnetic fields below 6 K for  $\text{Sr}_{0.5}\text{Pr}_{0.5}\text{FBiS}_2$  sample. As  $B = 0$  T, a sharp superconducting transition below 2.7 K is observed. With increasing magnetic field, the  $T_c$  is gradually suppressed and the superconducting transition becomes broader. For  $B = 1.5$  T, a tiny drop in resistivity at 0.9 K is still distinguishable. Further increasing the magnetic field to 9 T, the superconductivity disappears and resistivity recovers a weak semiconducting-like feature, similar to the case of  $\text{Bi}_4\text{O}_4\text{S}_3$  system.<sup>21</sup> The upper critical field  $\mu_0 H_{c2}(T)$  as a function of temperature is described in the inset of Fig.2(b), where  $T_c$  is determined by using 90% normal state resistivity criterion. According to the Ginzburg-Landau theory, the upper critical field  $\mu_0 H_{c2}$  with temperature follows the formula:  $H_{c2}(T) = H_{c2}(0)(1 - t^2)/(1 + t^2)$  where  $t$  is the renormalized temperature  $T/T_c$ . The upper critical field  $\mu_0 H_{c2}$  estimated is 1.9 T at  $T=0$  K, which is almost twice larger than that of  $\text{Sr}_{0.5}\text{La}_{0.5}\text{FBiS}_2$ ,<sup>7</sup> but still smaller compared with the Pauli paramagnetic limit  $\mu_0 H_p = 1.84T_c = 5$  T.

Figure 3 shows temperature dependence of magnetic susceptibility under 1 kOe for  $\text{Sr}_{0.5}\text{Pr}_{0.5}\text{FBiS}_2$ . The magnetic susceptibility does not display an anomaly associated with the local ferromagnetic or antiferromagnetic ordering of 4f electrons. In contrast, Ce-4f electrons can order ferromagnetically below 7.5 K in  $\text{Sr}_{0.5}\text{Ce}_{0.5}\text{FBiS}_2$  system.<sup>8</sup> The magnetic susceptibility seems to follow a modified Curie-Weiss behavior above 50 K with  $\chi = \chi_0 + C/(T - \theta)$ , where  $\chi_0$  denotes the temperature-independent term,  $C$  is the Curie-Weiss constant and  $\theta$  denotes the paramagnetic Curie temperature. By subtracting the temperature-independent term ( $\chi_0$ ), the  $(\chi - \chi_0)^{-1}$  shows a linear T-dependence above 50 K, suggesting a reliable fitting result. The fitting gives the effective magnetic moment of  $\mu_{eff}(\text{Pr}) = 3.8\mu_B/\text{Pr}$ , which is a little larger than the theoretical value of 3.57 for a free  $\text{Pr}^{3+}$  ion, and yields the Curie temperature of  $\theta = -32$  K. Noted that the long range magnetic ordering is absent in the other  $\text{BiS}_2$ -based superconductors, such as  $\text{LnO}_{1-x}\text{F}_x\text{BiS}_2$  ( $\text{Ln} = \text{Pr}, \text{Nd}$ )<sup>12</sup>

## B. Pressure effect

Temperature dependence of resistivity at various pressures is summarized in Figure 4. Fig. 4 (a) shows  $\rho(T)$  upon increasing pressure to 2.5 GPa. The semiconducting behavior is clearly observed at lower pressures, gradually suppressed with increasing pressure and finally turns to metallic at 2.5 GPa. Accompanied with a decrease of resistivity in the normal state, the  $T_c$  is enhanced under pressure. To clearly display the superconducting transition, an expanded view of resistivity around  $T_c$  is shown in fig.4 (b). For  $P \leq 0.8$  GPa,  $T_c^{\text{onset}}$ , which is determined as illustrated in fig.4 (b), has a slow increase with increasing pressure. As pressure is in the range 0.8 to 1.3 GPa, the superconducting transition broadens significantly, and two successive superconducting transitions for 1.15 GPa are detected at 5.5 K and 8.5 K, respectively. Further increasing pressure to 1.5 GPa, the transition becomes sharp again and  $T_c^{\text{onset}}$  is significantly enhanced to about 9 K. For higher pressure above 1.5 GPa,  $T_c^{\text{onset}}$  goes up slowly with pressure, and reaches 9.7 K at 2.5 GPa. The similar pressure effect was reported in the isostructure  $\text{EuFBiS}_2$ ,  $\text{LnO}_{1-x}\text{F}_x\text{BiS}_2$  and  $\text{LaO}_{1-x}\text{F}_x\text{BiSe}_2$  superconductors,<sup>13,22,23</sup> but the difference is remarkable. First, both  $\text{EuFBiS}_2$  and  $\text{LaO}_{1-x}\text{F}_x\text{BiSe}_2$  display a metallic behavior at ambient pressure. The metallicity of two systems can be enhanced under pressure. Second,  $\text{LaO}_{1-x}\text{F}_x\text{BiS}_2$  shows a weak semiconducting behavior at zero pressure, but still remains the semiconducting-like feature under pressure up to 3 GPa.<sup>13</sup>

In contrast, a semiconductor to metal transition can be observed with increasing pressure in the present  $\text{Sr}_{0.5}\text{Pr}_{0.5}\text{FBiS}_2$  sample. As shown in figure 4(c) and (d), at 1.0 GPa the resistivity exhibits a metallic behavior at high temperature, and then undergoes a metal to semiconductor transition around a characteristic temperature

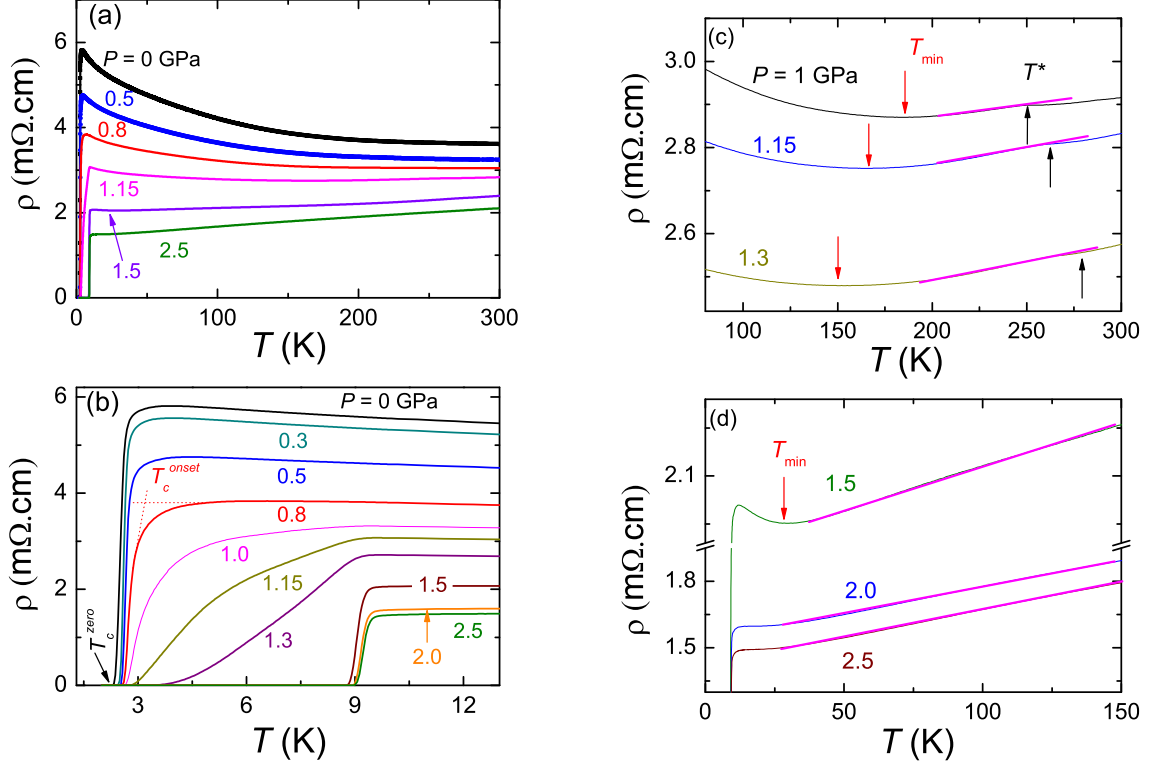


FIG. 4. (color online) (a) Temperature dependence of resistivity under several representative pressures for  $\text{Sr}_{0.5}\text{Pr}_{0.5}\text{FBiS}_2$  sample from 2 K to 300 K. (b) An enlarged view of superconducting transition in resistivity below 13 K. (c) and (d) enlarged plots of  $\rho(T)$  in the high temperature regime

$T_{min}$ . With further increasing pressure,  $T_{min}$  gradually shifts to lower temperature and finally vanishes above 1.5 GPa. The similar feature was reported in  $\text{Sr}_{1-x}\text{La}_x\text{FBiS}_2$  system, where the semiconductor-metal transition is induced by the La doping.<sup>11,24</sup> In particular, the first-principle calculation<sup>25</sup> has proposed that  $\text{LnO}_{1-x}\text{F}_x\text{BiS}_2$  will undergo a semiconductor-metal transition under pressure, but several experiments still fail to observe the transition even under very high pressures.<sup>13,14,16</sup> On the other hand, accompanied with the enhancement of metallicity under pressure, the resistivity obviously shows a linear temperature-dependent above  $T_{min}$ , which is different to the case of  $\text{EuFBiS}_2$  under pressure.<sup>22</sup> Noted that as pressure is in the range from 1.0 to 1.3 GPa, a kink in resistivity about 250 K, as illustrated in fig.4 (c), is clear observed. A similar feature was observed in the  $\text{EuFBiS}_2$  compound and was tentatively ascribed to the possible charge-density wave transition.<sup>26</sup>

According the above experimental results, the phase diagram of  $\text{Sr}_{0.5}\text{Pr}_{0.5}\text{FBiS}_2$  under pressure is summarized in Fig.5. For lower pressure,  $T_c$  has a slight increase with increasing pressure. As pressure crosses a critical value of  $P_c \simeq 1.5$  GPa,  $T_c$  dramatically increases from below 3 K to around 9 K, and a high- $T_c$  SC phase

emerges at higher pressure. Two distinct superconducting regions including the low- $T_c$  phase(SC1) below  $P_c$  so that the high- $T_c$  phase(SC2) above  $P_c$  are clearly distinguished, sharing a common feature in most  $\text{BiS}_2$ -based superconductors.<sup>13,15,22</sup> Such feature is likely related to the structure transition from a tetragonal phase to a monoclinic phase at a critical pressure ( $P_c$ ).<sup>16</sup> As a result, both the  $E_g$  and  $T_{min}$  decrease suddenly and then disappear across the critical pressure  $P_c$ . Noted that although the phase diagram in the superconducting state is similar to that observed in  $\text{EuFBiS}_2$ ,  $\text{Eu}_3\text{F}_4\text{Bi}_2\text{S}_4$  and  $\text{LaO}_{1-x}\text{F}_x\text{BiS}_2$  systems with a comparable  $T_c$  value at high pressure, the normal state in  $\text{Sr}_{0.5}\text{Pr}_{0.5}\text{FBiS}_2$  always undergoes a semiconductor to metal transition with pressure. Therefore, considering the robust semiconducting behavior against pressure and chemical element substitution in the  $\text{LnO}_{1-x}\text{F}_x\text{BiS}_2$  system, we believe that there is an essential difference in electronic property between  $\text{SrFBiS}_2$  and  $\text{LaOBiS}_2$ .

Fig.6(a) plots the temperature dependent resistivity under various magnetic field at highest pressure (2.5 GPa). For the zero magnetic field, a sharp superconducting transition with  $T_c$  of 9.7 K is observed. With the increase of magnetic field,  $T_c$  slightly shifts to lower

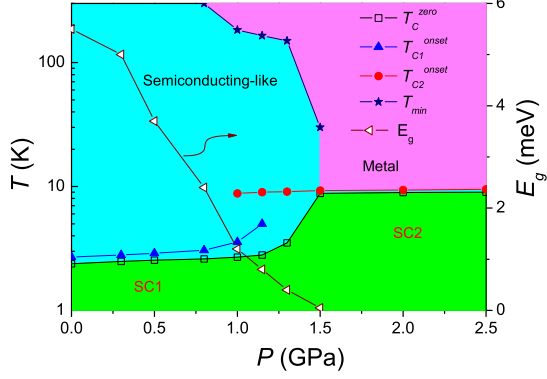


FIG. 5. (color online) Phase diagram of pressure vs. Temperature for  $\text{Sr}_{0.5}\text{Pr}_{0.5}\text{FBiS}_2$  sample.  $T_c^{\text{onset}}$  and  $T_c^{\text{zero}}$  represent the onset superconducting transition and zero resistivity in  $\rho(T)$ , respectively.  $T_{\text{min}}$  characterizes the semiconductor-metal transition from resistivity measurement. The thermal activation energy  $E_g$  is fitted for the temperature range from  $T_c$  to  $T_{\text{min}}$  by the mentioned formula in text.

temperatures and the transition gradually broadens. As magnetic fields exceed 4 T, a shoulder in  $\rho(T)$  curve is detected, as marked using arrow symbol in fig.6 (a). A similar character has been reported in the high pressure phase of  $\text{EuFBiS}_2$  and  $\text{Eu}_3\text{F}_4\text{Bi}_2\text{S}_4$ , which was interpreted as the anisotropy in the upper critical field. However, superconductivity seems to be rather robust keeping strong signals above 2 K even though the field is up to 9 T. As a comparison, in both  $\text{EuFBiS}_2$  and  $\text{Eu}_3\text{F}_4\text{Bi}_2\text{S}_4$  at high pressure,<sup>15,22</sup> a magnetic field of about 3.5 T can completely destroy superconductivity. The upper critical field is displayed in Fig.6(b), where the criterions of  $T_c^{\text{onset}}$  and  $T_c^{90\%}$  are employed to determined the  $\mu_0 H_{c2}$ . Its zero temperature limit estimated by the WHH formula  $H_{c2}(T) = -0.69T_c \left| \frac{\partial H_{c2}}{\partial T} \right|_{T_c}$  is about 25 T for  $T_c^{90\%}$ , which is over ten times larger than the value of  $\mu_0 H_{c2}(0) = 1.9$  T at  $P = 0$ . As a result, the value of  $B_{c2}(0)/T_c$  dramatically increases from 0.7 T/K at  $P = 0$  to 2.6 T/K at  $P = 2.5$  GPa, implying possible different origin of superconductivity in the corresponding superconducting phases. In contrast, the iso-structural  $\text{EuFBiS}_2$  has a comparable  $T_c$  of 9 K under 2.4 GPa, but its upper critical field is rather small, and  $B_{c2}(0)/T_c$  value abnormally decreases under pressure.<sup>22</sup> In addition, the positive curvature of  $H_{c2} - T$  diagram in the high- $T_c$  phase is clearly seen in the  $\text{Sr}_{0.5}\text{Pr}_{0.5}\text{FBiS}_2$ , indicative of the multi-band superconductivity.

#### IV. CONCLUSION

In summary, we have reported a newly  $\text{BiS}_2$ -based  $\text{Sr}_{0.5}\text{Pr}_{0.5}\text{FBiS}_2$  superconductor with  $T_c$  of 2.7 K by the

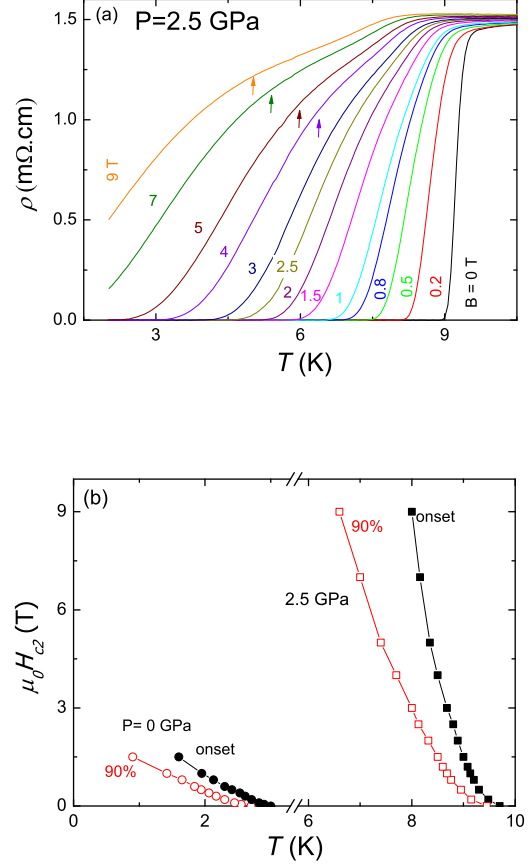


FIG. 6. (color online) (a) Superconducting transition vs.  $T$  under various magnetic fields at  $P = 2.5$  GPa. (b) Upper critical field  $\mu_0 H_{c2}(T)$ - $T$  phase diagram at ambient pressure and 2.5 GPa, respectively. The  $T_c^{\text{onset}}$  and  $T_c^{90\%}$  are determined from the onset superconducting transition and 90% of the normal state value in  $\rho(T)$ , respectively.

measurements of resistivity and magnetic susceptibility. We found that  $T_c$  is abruptly enhanced from below 2.7 K at ambient pressure to about 8.5 K at a critical pressure  $P_c = 1.5$  GPa, and finally reaches about 9.7 K at 2.5 GPa. Meanwhile, the normal state resistivity undergoes a semiconductor to metal transition under pressure, and both  $T_{\text{min}}$  and  $E_g$  decrease and almost approach to zero at  $P_c$ . The upper critical field ( $\mu_0 H_{c2}(0)$ ) estimated in the high- $T_c$  phase at 2.5 GPa is about 25 T, which exceeds the Pauli paramagnetic limit. The enhancement of  $\mu_0 H_{c2}(0)$  under pressure is over ten times larger than that of at ambient pressure. As a result, the ratio of  $B_{c2}(0)/T_c$  dramatically increases from 0.7 T/K at  $P = 0$  to 2.6 T/K at  $P = 2.5$  GPa. A tentative phase diagram with two distinct superconducting phases and a semiconductor-metal transition in the normal states is also plotted. All these results suggest that the two different superconducting phases may possess the different

origin and deserve to be investigated by further experiments.

## ACKNOWLEDGMENTS

This work is supported by the National Natural Science Foundation of China and National Training Programs of Innovation and Entrepreneurship for Undergraduates (201510346011).

## REFERENCES

- 
- <sup>1</sup> Y. Mizuguchi, H. Fujihisa, Y. Gotoh, K. Suzuki, H. Usui, K. Kuroki, S. Demura, Y. Takano, H. Izawa, O. Miura, Phys. Rev. B **86**, 220510(R) (2012).
  - <sup>2</sup> Y. Mizuguchi, S. Demura, K. Deguchi, Y. Takano, H. Fujihisa, Y. Gotoh, H. Izawa, O. Miura, J. Phys. Soc. Jpn. **81**, 114725 (2012).
  - <sup>3</sup> S. Demura, Y. Mizuguchi, K. Deguchi, H. Okazaki, H. Hara, T. Watanabe, S. J. Denholme, M. Fujioka, T. Ozaki, H. Fujihisa, Y. Gotoh, O. Miura, T. Yamaguchi, H. Takeya, and Y. Takano, J. Phys. Soc. Jpn. **82**, 033708 (2013).
  - <sup>4</sup> V. P. S. Awana, A. Kumar, R. Jha, S. Kumar, J. Kumar, and A. Pal, Solid State Communications **157**, 31 (2013).
  - <sup>5</sup> J. Xing, S. Li, X. Ding, H. Yang and H. H. Wen, Phys. Rev. B **86**, 214518 (2012).
  - <sup>6</sup> R. Jha, S. K. Singh, and V. P. S. Awana, J. Sup. and Novel Mag. **26**, 499 (2013).
  - <sup>7</sup> X. Lin, X. X. Ni, B. Chen, X. F. Xu, X. X. Yang, J. H. Dai, Y. K. Li, X. J. Yang, Y. K. Luo, Q. Tao, G. H. Cao, and Z. A. Xu, Phys. Rev. B **87**, 020504 (2013).
  - <sup>8</sup> L. Li, Y. K. Li, Y. F. Jin, H. R. Huang, B. Chen, X. F. Xu, J. H. Dai, L. Zhang, X. Yang, H. F. Zhai, G. H. Cao, and Z. A. Xu, Phys. Rev. B **91**, 014508 (2015).
  - <sup>9</sup> H. C. Lei, K. F. Wang, M. Abeykoon, E. S. Bozin, and C. Petrovic, Inorg. Chem. **52**, 10685 (2013).
  - <sup>10</sup> B. Li, Z. W. Xing, and G. Q. Huang, EPL **101**, 47002 (2013).
  - <sup>11</sup> Y. K. Li, X. Lin, L. Li, N. Zhou, X. F. Xu, C. Cao, J. H. Dai, L. Zhang, Y. K. Luo, W. H. Jiao, Q. Tao, G. H. Cao and Z. Xu, Supercond. Sci. Technol. **27**, 035009 (2014).
  - <sup>12</sup> D. Yazici, K. Huang, B. D. White, I. Jeon, V. W. Burnett, A. J. Friedman, I. K. Lum, M. Nallaiyan, S. Spagna, and M. B. Maple, Phys. Rev. B **87**, 174512 (2013).
  - <sup>13</sup> C. T. Wolowiec, D. Yazici, B. D. White, K. Huang, and M. B. Maple, Phys. Rev. B **88**, 064503 (2013).
  - <sup>14</sup> R. Jha, H. Kishan, and V. P. S. Awana, Solid State Communications **194**, 6 (2014).
  - <sup>15</sup> Y. K. Luo, H. F. Zhai, P. Zhang, Z. Xu, G. H. Cao, and J. D. Thompson, Phys. Rev. B **90**, 220510 (2014).
  - <sup>16</sup> T. Tomita, M. Ebata, H. Soeda, H. Takahashi, H. F. jihisa, Y. Gotoh, Y. Mizuguchi, H. Izawa, O. Miura, S. Demura, K. Deguchi, and Y. Takano, J. Phys. Soc. Jpn. **83**, 063704 (2014).
  - <sup>17</sup> C. T. Wolowiec, B. D. White, I. Jeon, D. Yazici, K. Huang, and M. B. Maple, J. Phys.: Condens. Matter **25**, 422201 (2013).
  - <sup>18</sup> B. Chen, C. Uher, L. Iordanidis, and M. G. Kanatzidis, Chem. Mater. **9**, 1655 (1997).
  - <sup>19</sup> J. Rajveer, T. Brajesh, and V. P. S. Awana, J. Appl. Phys. **117**, 013901 (2015).
  - <sup>20</sup> Y. Mizuguchi, H. Hiroi, J. Kajitani, H. Takatsu, H. Kadowaki, O. Miura, J. Phys. Soc. Jpn. **83**, 053704 (2014).
  - <sup>21</sup> S. Li, H. Yang, J. Tao, X. Ding, and H. H. Wen, Sci. China-Phys. Mech. Astron. **56**, 2019 (2014).
  - <sup>22</sup> C. Y. Guo, Y. Chen, M. Smidman, S. A. Chen, W. B. Jiang, H. F. Zhai, Y. F. Wang, G. H. Cao, J. M. Chen, X. Lu, and H. Q. Yuan, Phys. Rev. B **91**, 214512 (2015).
  - <sup>23</sup> J. Z. Liu, S. Li, Y. Li, X. Y. Zhu, H. H. Wen, Phys. Rev. B **90**, 094507 (2014).
  - <sup>24</sup> H. Sakai, D. Kotajima, K. Saito, H. Wadati, Y. Wakisaka, M. Mizumaki, K. Nitta, Y. Tokura, S. Ishiwata, J. Phys. Soc. Jpn. **83**, 014709 (2014).
  - <sup>25</sup> C. Morice, E. Artacho, S. Dutton, H. Kim, and S. Saxena, arXiv:1312.2615
  - <sup>26</sup> H. F. Zhai, Z. T. Tang, H. Jiang, K. Xu, K. Zhang, P. Zhang, J. K. Bao, Y. L. Sun, W. H. Jiao, I. Nowik, I. Felner, Y. K. Li, X. F. Xu, Q. Tao, C. M. Feng, Z. Xu, and G. H. Cao, Phys. Rev. B **90**, 064518 (2014).